ELSEVIER

Chemical Engineering Journal 73 (1999) 43–51

Chemical Engineering Journal

Effects of preparation variables of enzyme-encapsulating water-in-oil emulsion on enzymatic reaction conversion and emulsion stability in an enzyme–emulsion–liquid–membrane reactor

Jae Hwa Chang[a], Sang Cheol Lee[1,b,*], Won Kook Lee[c]

[a]*R & D Center, Sunkyong Engineering and Construction Ltd., Kwanhun Dong, Chongro Gu, Seoul 110-300, South Korea*
[b]*Department of Chemical Engineering, Kunsan National University, Miryong Dong, Kunsan, Chonbuk 573-701, South Korea*
[c]*Department of Chemical Engineering, Korea Advanced Institute of Science and Technology, Kusong Dong, Yusung Gu, Taejon 305-701, South Korea*

Received 15 March 1998; received in revised form 16 January 1999; accepted 24 January 1999

Abstract

The effects of various water-in-oil (W/O) emulsion preparation variables, such as water-to-oil volume ratio of W/O emulsion, emulsification speed and time, and emulsifying agent concentration, on the permeation rates of L-phenylalanine methyl ester (L-PME, substrate) and L-phenylalanine (L-Phe, product) were investigated in an enzyme–emulsion–liquid–membrane (EELM) system accompanying the hydrolysis of the substrate into the product. The permeation rate of the substrate was higher in the system with a higher water-to-oil volume ratio or lower emulsification energy, while emulsifying agent concentration had little influence on its permeation rate as far as emulsion was stable. The permeation rate of the product was highest in the system with water-to-oil ratio of 1/1, the lowest emulsification energy or 7 wt.% emulsifying agent concentration. This is because the rate was dependent only on the mass transfer resistance, such as surfactant layer resistance at interfaces, membrane thickness, and the mass transfer area between external phase and emulsion drops. The explanation was supported by the experimentally measured data of emulsion drop size, emulsion viscosity, and internal droplet size. Finally, the optimum permeation rate was obtained at 7 wt.% emulsifying agent concentration, water-to-oil volume ratio of 1/1 and emulsification speed of 6000 rpm for 15 min.

Keywords: Enzyme–emulsion–liquid–membrane; Water-to-oil volume ratio; Emulsification energy; Emulsifying agent concentration; Emulsion drop size

1. Introduction

The emulsion liquid membrane (ELM), which was first developed by Li in 1968 [1], offers an effective means of encapsulating materials and separating mixtures. This technique has shown considerable promise in a variety of separations which include separation of hydrocarbons, wastewater treatment, recovery and purification of metal ions, and applications in biochemical and biomedical fields [2–8]. Among the biochemical applications, the ELMs have potential utility as membrane reactors incorporating simultaneous separation and enzymatic reaction processes [9–11]. These processes are carried out by encapsulating enzymes within water-in-oil (W/O) emulsion and dispersing the emulsion in a continuous reactant phase. These provide non-permanent immobilization techniques of biocatalyst, and the reactor working with the enzyme emulsion is called enzyme–emulsion–liquid–membrane (EELM) reactor [12]. The enzyme can be easily immobilized within the desired emulsion in the EELM reactor and recovered for reuse by simple disruption of the emulsion. The liquid membrane in the EELM reactor makes it possible to protect the immobilized enzyme from inhibitors, which enables the enzymatic reaction step to be integrated with downstream processing. In complex fermentation broth, a desired substrate also can be preselected by right choice of the membrane.

Although the EELM technique has several advantages over other enzyme immobilization techniques, some problems remain to be solved in order to apply the EELM to a practical process. Especially, it is required that enzyme activity and emulsion stability must be almost unchanged throughout continuous operation. In general, the emulsion stability in the EELM system is decreased by membrane breakage and swelling. The membrane breakage includes rupture of the emulsion, leading to loss of enzyme. As a result, the breakage makes it impossible to encapsulate enzyme within the emulsion. The main factors affecting

*Corresponding author. Tel.: +1-805-893-4363; fax: +1-805-893-4731; e-mail: lee40f@engineering.ucsb.edu

[1]Department of Chemical Engineering, University of California, Santa Barbara, CA 93106-5080, USA.

1385-8947/99/$ – see front matter
PII: S1385-8947(99)00037-6

the emulsion stability encompass membrane formulation, method of emulsion preparation, and the condition under which the emulsion is contacted with a reactant phase. Swelling is the phenomenon by which water is transported from external phase to internal phase and is mainly driven by the difference in osmotic pressure between the external and the internal phases. The water transfer will (1) reduce the driving force for substrate consumption; (2) make the membrane thinner, thereby, leading to a less stable emulsion; and (3) change rheological properties of the emulsion to cause difficulties in emulsion transportation and phase separation [13,14]. In consequence, the changes in the emulsion properties increase the agitation power required to disperse the emulsion, making it difficult to perform continuous operation.

Composition of emulsion and method of emulsion preparation significantly affect enzymatic reaction rate as well as emulsion stability. There are several operating variables to dominate the emulsion characteristics in the EELM system regardless of the type of the enzymatic reaction: water-to-oil volume ratio of the W/O emulsion, emulsification speed, emulsification time and emulsifying agent concentration. However, few researchers have studied the influences of those variables on the EELM performance in the aspect of practical application.

In this work we, therefore, investigated the effects of the preparation conditions of the emulsion on the enzymatic reaction rate and the emulsion stability in an EELM reactor. The results were elucidated with the help of more detailed information on the emulsion such as emulsion drop size, emulsion viscosity and the droplet size of internal aqueous phase, etc. The hydrolysis of L-phenylalanine methyl ester (L-PME) into L-phenylalanine (L-Phe) mediated by α-chymotrypsin was chosen as the model reaction of the EELM system [12]. This enzymatic reaction is closely related to the stereoselective hydrolysis of DL-phenylalanine methyl ester (DL-PME) into L-Phe, which has significance on the optical resolution of racemic mixtures [15]. Finally, this work can provide a guideline for applying the EELM system to practical enzymatic reaction processes by ultimately giving the criteria of optimum conditions for the emulsion preparation.

2. Experimental

2.1. Materials

L-PME, L-Phe and enzyme α-chymotrypsin were supplied from Sigma (USA). Kerosene was purchased from Kanto (Japan), and its specific gravity was 0.78 at 20°C. Paranox 100 was a polyamine-type surfactant obtained from Exxon. Adogen 464 was purchased from Aldrich, and its main composition was tri-octyl-methyl ammonium chloride (TOMAC).

2.2. Method

The organic solution, used as the membrane phase of the EELM system, was prepared by dissolving Paranox 100 and Adogen 464 in kerosene. The aqueous phosphate buffer solution, in which α-chymotrypsin was dissolved, was used as the internal phase. To prepare the enzyme-encapsulating emulsion, the aqueous enzyme solution was added slowly to the organic solution with mixing provided by a high-speed homogenizer (Tekmar, Germany), and it was dispersed in the organic solution to form small aqueous droplets. A substrate solution was the aqueous phosphate buffer solution in which L-PME was dissolved. For the EELM experiment, the prepared W/O emulsion was dispersed in the aqueous substrate solution which was the external phase of the EELM system. The EELM experiments were carried out in a 750 ml reactor fitted with four vertical baffles so as to prevent vortex during mixing of the aqueous substrate solution and the emulsion. Simultaneously, isothermal condition (25°C) was maintained in the system with a water jacket around the reactor.

The enzymatic reaction in the EELM system was the hydrolysis reaction of L-PME into L-Phe over the enzyme α-chymotrypsin and is expressed as follows:

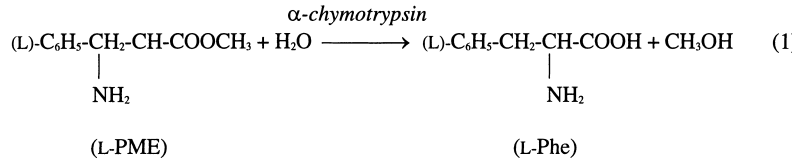

(1)

The substrate (L-PME) in the external phase diffuses through the membrane phase by a physical solubility, while the product (L-Phe) diffuses back with aid of the carrier (Adogen 464, quaternary ammonium salts) after it is generated in the internal phase. The detailed transport mechanism was described in our previous work [12]. Fig. 1 shows the schematic diagram of the transport mechanism of L-PME and L-Phe in the EELM system accompanying the enzymatic reaction.

In order to measure the extent of enzymatic reaction conversion, samples were periodically taken from the reactor, and then the external solution was separated from the emulsion phase by filtering with a membrane-filter (Millipore). The concentrations of L-PME and L-Phe in the external solution were determined by HPLC (Waters) using μ-Bondapak C_{18} column.

Observation of emulsion drops was made using a camera (Nikon) equipped with a microscope with the help of an illuminator (Fiber-Lite, Bausch and Lomb, Germany). The

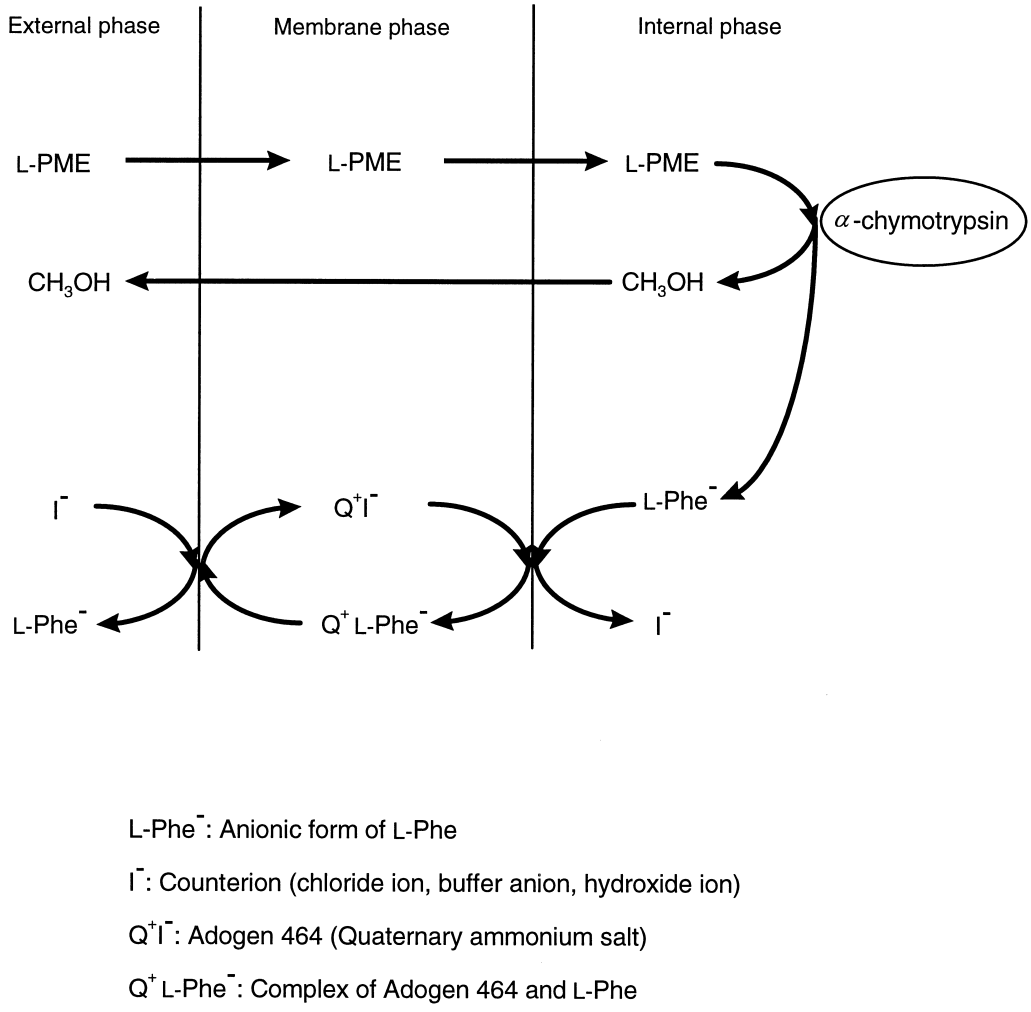

Fig. 1. Schematic diagram of the transport mechanism of the substrate (L-PME) and the product(L-Phe) in the EELM system.

photographs were taken with the shutter speed of 1/4000 s. In addition, a centrifugal particle size analyzer (Shimadzu SA-CP3) was used to obtain the size distribution of the internal droplets, and the viscosity of the emulsion at 25°C was determined using a digital viscometer (Brookfield Model DV-II).

The extent of membrane breakage could be determined from the amount of enzyme in the external phase leaked from the internal phase. In other words, it was easily evaluated by seeing how far the enzymatic reaction proceeded when the fresh substrate was added to the external phase. This method has the advantage of precluding the use of a tracer which may have influence on the EELM system.

For testing emulsion swelling, we observed the change in the sizes of the emulsion drops by taking photographs. The swelling percentage of the emulsion is defined as the ratio of the volume increment at any time to the initial volume of the emulsion phase and is as follows:

$$E_s = \frac{V_{em} - V_{em,0}}{V_{em,0}} \times 100(\%) \quad (2)$$

Fig. 2 summarizes the overall procedure of the EELM experiment schematically. Table 1 gives the typical experimental conditions in the EELM experiment.

Table 1
Typical experimental condition in the EELM system

Internal phase
α-chymotrypsin 2.0 g/l
pH to 7.0 with phosphate buffer
Membrane phase
Kerosene 92 wt.%
Paranox 100 7 wt.%
Adogen 464 1 wt.%
External phase
L-PME 10 mM
pH to 7.0 with phosphate buffer
Water-to-oil volume ratio of W/O emulsion 1/1
External-to-emulsion volume ratio 4.8
Emulsification speed 11 000 rpm
Emulsification time 15 min
Temperature 25°C
Stirrer speed 300 rpm

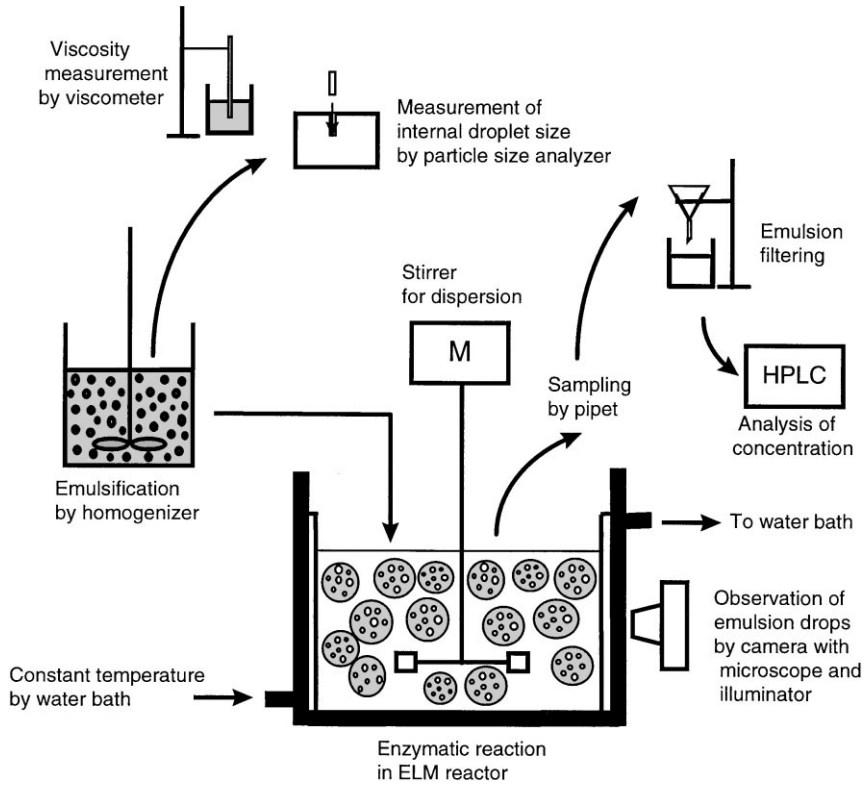

Fig. 2. Schematic diagram of overall procedure for the EELM experiment.

3. Results and discussion

3.1. Effect of water-to-oil volume ratio of W/O emulsion

The correlation between water-to-oil volume ratio of W/O emulsion ($\phi_{W/O}$) and emulsion viscosity was investigated in order to understand the EELM system better. As shown in Fig. 3(a), the increase in $\phi_{W/O}$ in the range of $\phi_{W/O}$ above 1.0 led to a drastic increase in the emulsion viscosity at the high shear rate (79.2 s^{-1}). Very dilute emulsions ($\phi_i < 0.1$) behave like simple liquids and exhibit Newtonian flow. In case of more concentrated emulsions ($\phi_i > 0.5$), internal droplets interact with one another and flocculate to form the aggregates which show viscoelastic behavior. The relative viscosity of a dilute emulsion is defined in terms of viscosity of continuous oil phase (η_o) and internal droplet volume fraction (ϕ_i) by using the following equation proposed by Einstein [16,17],

$$\eta_{rel} = \frac{\eta}{\eta_o} = 1 + 2.5\phi_i \quad (3)$$

provided there is no interaction between the internal droplets, and η rises from the dissipation energy, or viscous drag, produced by modification to fluid motion near the droplet interfaces.

Fig. 3(b) shows the effect of water-to-oil volume ratio on the relative emulsion viscosity measured at the high shear rate. When ϕ_i increases beyond the limits of validity of

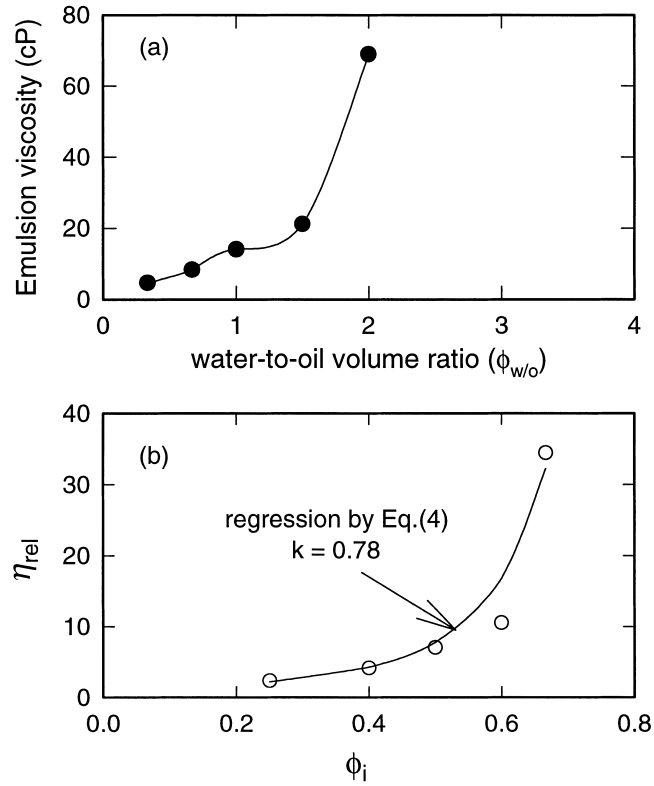

Fig. 3. Effect of water-to-oil volume ratio on emulsion viscosity measured at the shear rate of 79.2 s^{-1}; (a) Emulsion viscosity versus water-to-oil volume ratio. (b) Relative emulsion viscosity versus volume fraction of internal phase.

Eq. (3), the distorted flow patterns around the droplets draw close together and eventually they overlap. The resulting hydrodynamic interaction increases ϕ_{rel}. The viscosities of concentrated emulsions at the high shear rate such that the droplets are completely deflocculated can be satisfactorily described by the following relation [18]:

$$\frac{\eta_\infty}{\eta_o} = \exp\left(\frac{2.5\phi_i}{1 - k\phi_i}\right) \quad (4)$$

where k depends on the hydrodynamic interaction between the droplets. The k value estimated by fitting data of Fig. 3 to Eq. (4) was 0.78.

The mass transfer area between the external phase and the emulsion drops functions as one of the most important factors affecting the permeation rates of the substrate and the product in the EELM system. It is also in close connection with the average size of the emulsion drops, which depends on the emulsion viscosity having functional relation with $\phi_{W/O}$. In order to illuminate the effect of $\phi_{W/O}$ on the permeation rates, it is therefore necessary to express the mass transfer area using Sauter mean diameter which characterizes the average size of the emulsion drops.

For two EELM systems having only different water-to-oil volume ratios, the mass transfer areas, that is, the outer surface areas of the emulsion drops, A_{e1} and A_{e2} can be expressed using Sauter mean diameters, $d_{32,1}$ and $d_{32,4}$ by following equations, respectively:

$$A_{e1} = \pi d_{32,1}^2 N_1 \quad (5)$$

$$A_{e2} = \pi d_{32,1}^2 N_2 \quad (6)$$

where N_1 and N_2 are numbers of the emulsion drops. When the volumes of the emulsion phase for the two systems are equal and the change in the emulsion volume such as emulsion swelling can be ignored, the emulsion volumes can be expressed by

$$(V_m + V_i)_1 = \frac{\pi d_{32,1}^3}{6} N_1 = (V_m + V_i)_2 = \frac{\pi d_{32,2}^3}{6} N_2 \quad (7)$$

Eq. (5) through Eq. (7) give the following relationship:

$$\frac{A_{e1}}{A_{e2}} = \frac{d_{32,2}}{d_{32,1}} \quad (8)$$

In consequence, the ratio between two mass transfer areas is inversely proportional to the ratio between two Sauter mean diameters. Fig. 4 gives the effect of $\phi_{W/O}$ on emulsion drop size distribution. Table 2 shows Sauter mean diameters of the internal phase droplets and the emulsion drops, and the swelling percentage of the emulsion for all the experimental conditions. As shown in Fig. 4 and Table 2, a higher $\phi_{W/O}$, on the whole, caused a larger average size of the emulsion drops and wider size distribution, and thus brought about a smaller mass transfer area.

Fig. 5 shows the effect of $\phi_{W/O}$ on the changes in the normalized concentrations of L-PME (substrate) and L-Phe

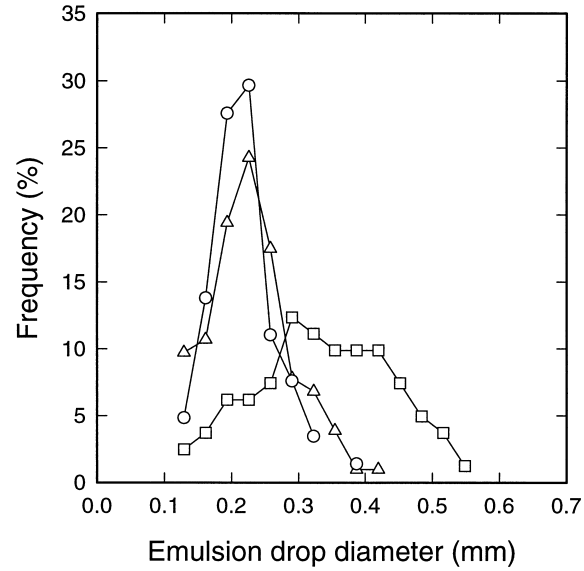

Fig. 4. Size distribution of emulsion drops at the following water-to-oil volume ratio: △, 1/3; ○, 1/1; □, 2/1.

(product) in the external phase with time, which are defined as the ratios of the substrate and the product concentrations at any time elapsed to an initial substrate concentration, respectively. The substrate concentration in the external phase decreased more rapidly with time at a higher $\phi_{W/O}$, because the substrate transported into the internal phase was exhausted faster, due to a larger enzyme amount in the internal phase so that the substrate concentration gradient between the external and the internal phases continued to be maintained more highly. This implies that the permeation rate of the substrate strongly depends on the enzyme mass of the internal phase as a sink for the substrate rather than the outer surface area between the external phase and the

Table 2
Emulsion property data of each system

System	$d_{32,i}$ (μm)[a]	$d_{32,em}$ (mm)[b]	E_s[c] (%)
A	2.01	0.24	9
B	1.01	0.26	4
C	4.11	0.42	19
D	4.31	0.22	10
E	1.12	0.34	30
F	1.51	–[d]	–[d]
G	1.86	0.38	35

System A: $\phi_{W/O}$: 1/1, C_s: 7 wt.%, emulsify 15 min at 11 000 rpm
System B: $\phi_{W/O}$: 1/3, C_s: 7 wt.%, emulsify 15 min at 11 000 rpm
System C: $\phi_{W/O}$: 2/1, C_s: 7 wt.%, emulsify 15 min at 11 000 rpm
System D: $\phi_{W/O}$: 1/1, C_s: 7 wt.%, emulsify 15 min at 6700 rpm
System E: $\phi_{W/O}$: 1/1, C_s: 7 wt.%, emulsify 30 min at 11 000 rpm
System F: $\phi_{W/O}$: 1/1, C_s: 5 wt.%, emulsify 15 min at 11 000 rpm
System G: $\phi_{W/O}$: 1/1, C_s: 10 wt.%, emulsify 15 min at 11 000 rpm
[a] Measured after preparing emulsion.
[b] Taken by photograph at about 30 min.
[c] Measured after 2 h operation.
[d] Could not be measured due to emulsion breakage.

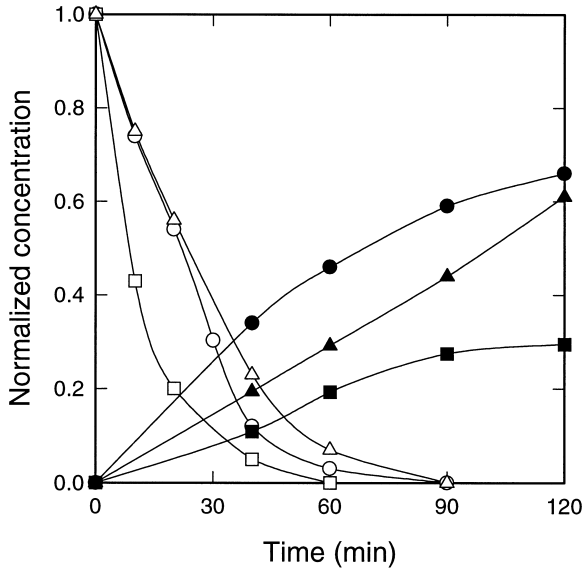

Fig. 5. Concentration profiles of L-PME (hollow symbol) and L-Phe (filled symbol) in the external phase at the following water-to-oil volume ratio: △, 1/3; ○, 1/1; □, 2/1.

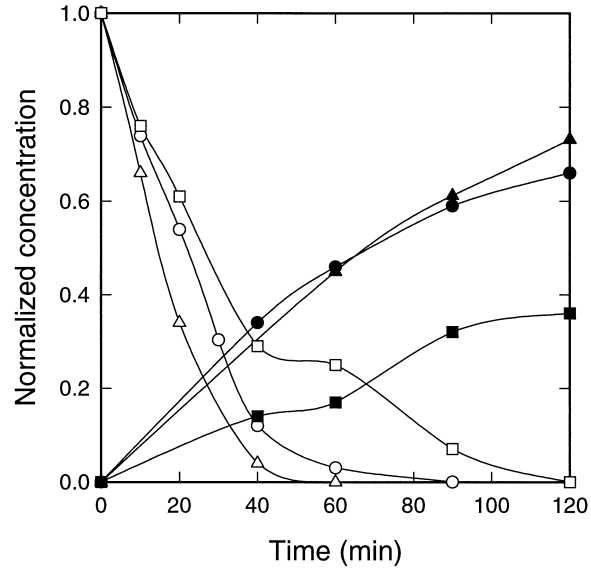

Fig. 7. Concentration profiles of L-PME (hollow symbol) and L-Phe (filled symbol) in the external phase at the following emulsification speed and time: △, 6700 rpm, 15 min.; ○, 11 000 rpm, 15 min; □, 11 000 rpm, 30 min.

emulsion drops. Generally, diffusional resistance through the membrane phase decreases with $\phi_{W/O}$ due to a decrease in membrane thickness while the outer surface area decreases with it. Finally, we could note that such contrary effects on permeation resulted in the highest permeation rate of the product at $\phi_{W/O}$ of 1/1, as shown in Fig. 5.

The dependence of internal droplet size distribution on $\phi_{W/O}$ is displayed in Fig. 6, indicating that the average size of the internal droplets increases with increasing $\phi_{W/O}$, as described in Table 2. However, it is known that the difference in the average size of the internal droplets usually have a little influence on a permeation rate of a solute, because their sizes are very small independent of $\phi_{W/O}$ and, thus, the mass transfer resistance around the interface between the membrane phase and the internal phases is negligible compared with other resistances [19].

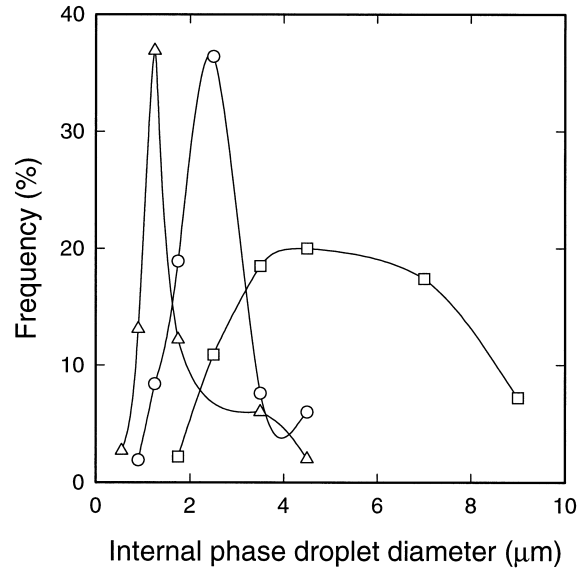

Fig. 6. Size distribution of internal phase droplets at the following water-to-oil volume ratio: △, 1/3; ○, 1/1; □, 2/1.

3.2. Effect of emulsification speed and emulsification time

The energy input dissipated during emulsification depends on emulsification speed and time. We investigated their effects on the concentration changes in the substrate and the product in the external phase. Fig. 7 shows that as the energy input to the system was larger due to the faster emulsification speed and the longer agitated time, the permeation rates of the substrate and the product were lower. This result can be attributed to a decrease in enzyme activity due to the loading of higher shear energy to the emulsion, and the decrease in outer surface area of the emulsion drops resulting from the increase in emulsion drop size, as shown in Fig. 8. The reason for the increase in the emulsion drop size can be explained as follows.

The higher emulsification energy brought about a smaller internal droplet size, as displayed in Fig. 9. When the internal droplet size is smaller, for a given concentration of emulsifying agent in the membrane phase, the emulsifying agent is distributed over a greater interfacial area at the interface between the internal and the emulsion phases, which reduces the density of surfactant barrier at the interface between the external and the emulsion phases and leads to a corresponding increase in interfacial tension [19]. Finally, the outer surface area created becomes smaller for the emulsions with higher interfacial tension when stirrer speed is held constant.

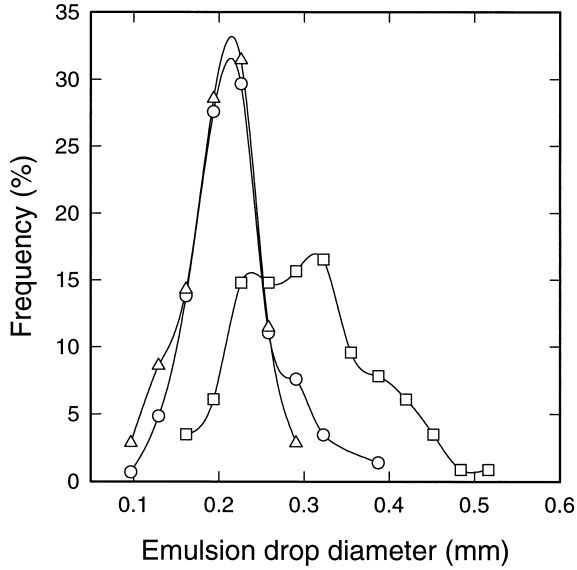

Fig. 8. Size distribution of emulsion drops at the following emulsification speed and time: Δ, 6700 rpm, 15 min; ○, 11 000 rpm, 15 min; □, 11 000 rpm, 30 min.

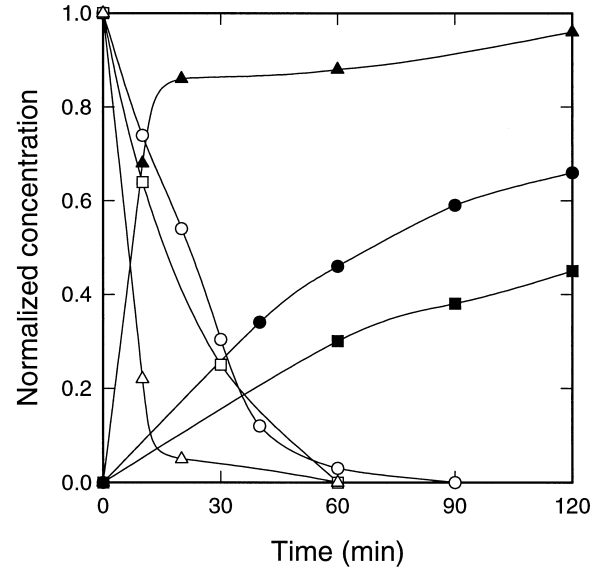

Fig. 10. Concentration profiles of L-PME (hollow symbol) and L-Phe (filled symbol) in the external phase at the following emulsifying agent concentration: Δ, 5 wt.%; ○, 7 wt.%; □, 10 wt.%.

Emulsion swelling was considerable in the EELM system with emulsions prepared at the higher emulsification speed and the longer emulsification time (See Table 2). This results from the decrease in the permeation rate of the product from the internal to the external phase. In other words, the product is less released from the internal phase and is more accumulated there so that the difference in osmotic pressure across the membrane phase is increased [20].

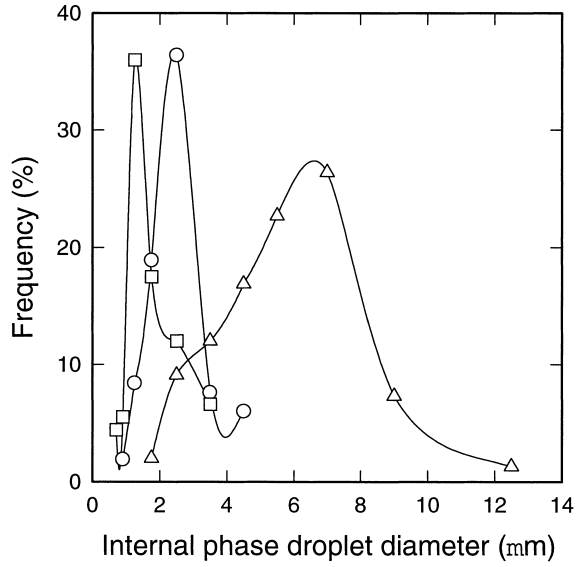

Fig. 9. Size distribution of internal phase droplets at the following emulsification speed and time: Δ, 6700 rpm, 15 min; □, 11 000 rpm, 15 min; ○, 11 000 rpm, 30 min.

3.3. Effect of emulsifying agent concentration

Fig. 10 shows the variation in the permeation rates of the substrate and the product with changing the concentration of Paranox 100 as the emulsifying agent in the membrane phase, which is defined as the ratio of the weight of Paranox 100 dissolved in the membrane phase to that of the membrane phase on a percentage basis.

The permeation rates of the substrate and the product was very high at 5 wt.% emulsifying agent concentration, as shown in Fig. 10. This result can be attributed to the breakage of the emulsion. The breakage was identified by the addition of a quantity of substrate to the external phase after separating the external and the emulsion phases in 120 min. Then the conversion of L-PME to L-Phe was made within a short time only at 5 wt.% emulsifying agent concentration, because considerable parts of α-chymotrypsin in the internal phase were leaked to the external phase. Such demonstration is elucidated well by Fig. 11 which gives the influence of the emulsifying agent concentration on internal droplet size distribution. Fig. 11 shows that the size distribution of the internal droplets was almost independent of the initial emulsifying agent concentration in the membrane phase. From the fact, we could note that amounts of the emulsifying agent at the interface between the membrane and the internal phases were almost the same for all the initial emulsifying agent concentration. Simultaneously, the density of the emulsifying agent at the interface between the external phase and the emulsion drops was supposed to become smaller at a lower emulsifying agent concentration during the formation of temporary double water-in-oil-in-water emulsions. Finally, in case of 5 wt.% emulsifying agent concentration the smallest density of the emulsifying

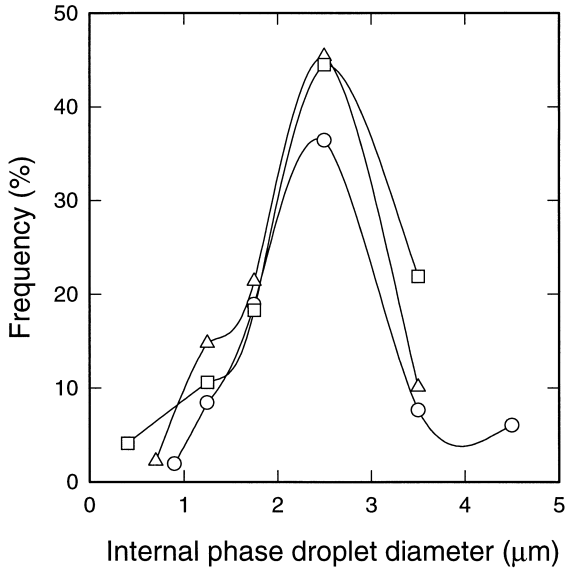

Fig. 11. Size distribution of internal phase droplets at the following emulsifying agent concentration: △, 5 wt.%; ○, 7 wt.%; □, 10 wt.%.

agent at the interface could be considered to bring about the instability of the emulsion.

The permeation rate of the product at 10 wt.% emulsifying agent concentration was lower than that at 7 wt.% as shown in Fig. 10, which could be ascribed to two reasons. First, the average size of the emulsion drops was larger due to a higher viscosity at the higher emulsifying agent concentration as shown in Fig. 12. The increase in the average size brought about a decrease in mass transfer area. Secondly, the higher emulsifying agent concentration resulted in the larger mass-transfer resistance coming from the formation of thicker surfactant adsorption layers at the interfaces.

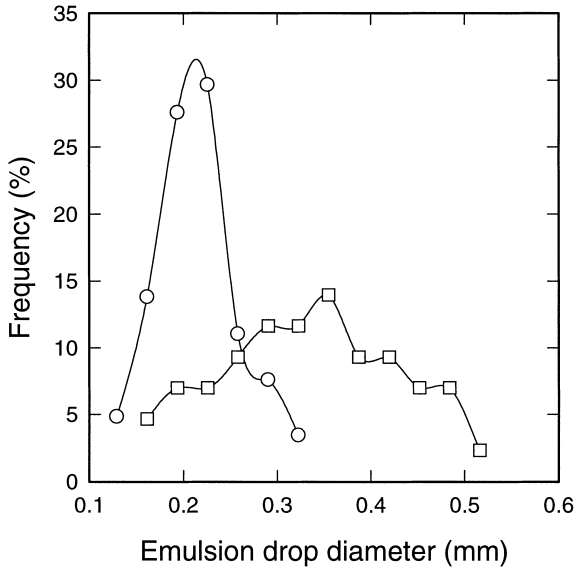

Fig. 12. Size distribution of emulsion drops at the following emulsifying agent concentration: ○, 7 wt.%; □, 10 wt.%.

The permeation rates of the substrate between 7 and 10 wt.% emulsifying agent concentrations was almost the same, as shown in Fig. 10. It can be supposed that more reversed micelles formed by the emulsifying agent can contribute for the transport of the substrate at the higher emulsifying agent concentration. At 10 wt.% emulsifying agent concentration, such effect seems to be offset by the decrease in the permeation rate of the substrate owing to the increases in the emulsion drop size and the interfacial resistance described above.

4. Conclusions

The effects of W/O emulsion preparation variables on the permeation rates of the substrate (L-PME) and the product (L-Phe) in an EELM reactor were studied with the help of a more detailed emulsion information such as emulsion drop size, emulsion viscosity and the droplet size of internal aqueous phase of W/O emulsion. The hydrolysis of the substrate into the product catalyzed by α-chymotrypsin was chosen as the model reaction of the EELM system. Emulsion preparation variables include water-to-oil volume ratio ($\phi_{W/O}$) of W/O emulsion, emulsification speed, emulsification time, and concentration of emulsifying agent.

The permeation rate of the substrate in the external phase was higher at a higher $\phi_{W/O}$ because of its strong dependence on the enzyme amount in the internal phase. On the other hand, the permeation rate of the product to the external phase was highest at $\phi_{W/O}$ of 1/1. This can be ascribed to two contrary effects on the product permeation, the increase in membrane thickness and the decrease in emulsion drop size with decreasing $\phi_{W/O}$. We could also conclude that the product permeation in the EELM reactor was mostly governed by diffusion through the emulsion drop independent of the internal droplet size.

As higher emulsification energy was put into the EELM system, both the permeation rates of the substrate and the product were lower. The higher emulsification energy brings about the decrease in surfactant concentration at the interface between the external phase and the emulsion drops due to the formation of smaller internal droplets. Finally, larger emulsion drops are formed to reduce the outer surface area of the emulsion drops. Also, the swelling at the higher emulsification energy was considerable because the permeation rate of the product was lower at the higher energy.

A 5 wt.% emulsifying agent concentration resulted in the instability of the emulsion. Also, the permeation rate of the product at 10 wt.% emulsifying agent concentration was lowest because of the increase in the emulsion drop size and the formation of thicker surfactant layers at the interfaces. Finally, an optimal emulsifying agent concentration of 7 wt.% was obtained.

5. Nomenclature

A_e outer surface area of W/O emulsion (m^2)
d_{32} Sauter mean diameter (m)
E_s swelling percentage of emulsion defined by Eq. (2)
k hydrodynamic interaction parameter in Eq. (4)
N number of emulsion drops
V_{em} volume of emulsion at any time t, $V_i + V_m(m^3)$
$V_{em,0}$ volume of emulsion at time $t = 0$, (m^3)
V_i volume of internal phase (m^3)
V_m volume of membrane phase (m^3)

Greek letters

ϕ_i volume fraction of internal phase in W/O emulsion, V_i/V_{em}
$\phi_{W/O}$ volume ratio of aqueous internal phase to oil membrane phase, V_i/V_m
η viscosity of emulsion (cP)
η_o viscosity of continuous oil phase (cP)
η_{rel} relative viscosity of emulsion defined by Eq. (3)
η_∞ viscosity of emulsion at high shear rates (cP)

Acknowledgements

The authors are grateful to Exxon Chemical Company for the supply of Paranox 100.

References

[1] N.N. Li, US Patent No. 3,410,794, 1968.
[2] T.C.S.M. Gupta, A.N. Goswami, B.S. Rawat, J. Membr. Sci. 54 (1990) 119.
[3] W.S. Ho, T.A. Hatton, E.N. Lightfoot, N.N. Li, Am. Inst. Chem. Eng. J. 28 (1982) 66.
[4] S.C. Lee, B.S. Ahn, W.K. Lee, J. Membr. Sci. 114 (1996) 171.
[5] M.P. Thien, T.A. Hatton, Sep. Sci. Technol. 23 (1988) 819.
[6] S.C. Lee, W.K. Lee, J. Chem. Tech. Biotechnol. 55 (1992) 251.
[7] S.C. Lee, K.H. Lee, G.H. Hyun, W.K. Lee, J. Membr. Sci. 124 (1997) 43.
[8] J.B. Chaudhuri, D.L. Pyle, Chem. Eng. Sci. 47 (1992) 41.
[9] R.R. Mohan, N.N. Li, Biotechnol. Bioeng. 17 (1975) 1137.
[10] T. Scheper, Z. Likidis, K. Makryaleas, C. Nowottny, K. Schügerl, Enzyme Microb. Technol. 9 (1987) 625.
[11] H.Y. Ha, S.A. Hong, Biotechnol. Bioeng. 39 (1992) 125.
[12] J.H. Chang, W.K. Lee, Chem. Eng. Sci. 48 (1993) 2357.
[13] S. Matsumoto, T. Inoue, M. Kohda, K. Ikura, J. Colloid Interface Sci. 77 (1980) 555.
[14] H. Itoh, M.P. Thien, T.A. Hatton, D.I.C. Wang, J. Membr. Sci. 51 (1990) 309.
[15] S.B. Mirviss, S.K. Dahod, M.W. Empie, Ind. Eng. Chem. Res. 29 (1990) 651.
[16] A. Einstein, Ann. Phys. 19 (1906) 289.
[17] A. Einstein, Ann. Phys. 24 (1911) 591.
[18] P. Sherman, in: P. Becher (Ed.), Encyclopedia of Emulsion Technology, vol. 1, Marcel Dekker, New York, 1983, p. 405.
[19] R. Chakraborty, S. Datta, J. Membr. Sci. 96 (1994) 233.
[20] C. Schöller, J.B. Chaudhuri, D.L. Pyle, Biotechnol. Bioeng. (1993) 50.